

## Auto-Zero Amplifiers

The Ideal Choice for High-Gain Sensor Signal Amplifiers

### Abstract

Many sensor signal amplifiers deal with the conditioning of extremely small input signals. Their high signal gain requires signal paths with extremely low offset voltage and low offset voltage drift over time and temperature, as well as high gain accuracy. To satisfy these requirements with standard linear components requires system-level auto-calibration and multi-stage amplifiers. This, however, complicates the hardware and software design, increases the design cost, and slows down time-to-market for new products.

The alternative is to use components with low offset and drift and high open-loop gain ( $A_{OL}$ ) for high gain accuracy. The amplifier with by far the highest  $A_{OL}$  and lowest offset and drift is an auto-zero amplifier, such as the Renesas ISL28134. This amplifier achieves high DC precision through a continuously running calibration mechanism that is implemented on-chip. With typical values of 0.2 $\mu$ V input offset, and 0.5nV/ $^{\circ}$ C offset drift over-temperature drift, the ISL28134 satisfies even the highest requirements of DC accuracy.

This tech brief explains the auto-zero calibration technique and compares the noise spectrum of the ISL28134 with that of a standard CMOS op-amp. Four application examples demonstrating the use of the ISL28134 as a thermocouple amplifier, and as a calibrating amplifier in DC - and wideband AC - applications, conclude this tech brief.

### Contents

<b>1. The Auto-Zero Amplifier</b>	<b>2</b>
<b>2. Noise Reduction in the Frequency Domain</b>	<b>3</b>
<b>3. Applications</b>	<b>5</b>
3.1 Thermocouple Amplifier	5
3.2 Active Low-Pass Filter	5
3.3 Wideband Amplifier	5
3.4 High-Gain Amplifier	6
<b>4. Conclusion</b>	<b>7</b>
<b>5. Revision History</b>	<b>7</b>

### List of Figures

Figure 1. ISL28134: Nulling or Auto-zeroing Phase	2
Figure 2. ISL28134: Amplification Phase	2
Figure 3. Generic Amplifier with Effective Offset	3
Figure 4. Auto-Zeroing in the Frequency Domain	4
Figure 5. Spectral Noise Density	4
Figure 6. Temperature Measurement with Thermocouple	5
Figure 7. 200kHz 3rd Order Low-pass Filter	5
Figure 8. Auto-Zeroed Wideband Amplifier	6
Figure 9. Making $R_S  R_I = R_F  R_G$ Reduces Input Offset Voltage Due to Bias Currents	7
Figure 10. ISL28134: Block Diagram and Key Features	7

### Related Literature

For a full list of related documents, visit our website:

- [ISL28134](#) device page

# 1. The Auto-Zero Amplifier

Figure 1 shows the principle structure of an auto-zero amplifier. Here, a wideband main amplifier ( $A_M$ ) is offset-corrected by a parallel nulling amplifier ( $A_N$ ). Offset correction of the overall amplifier occurs within one cycle of the auto-zero clock frequency ( $f_{AZ}$ ) and is split into two modes of operation: an auto-zero phase and an amplification phase.

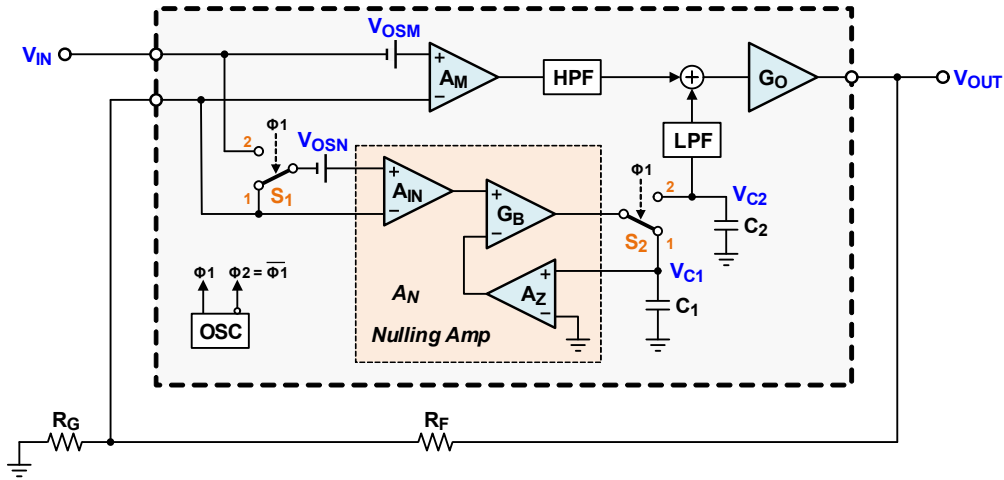


Figure 1. ISL28134: Nulling or Auto-zeroing Phase

The oscillator (OSC) generating  $f_{AZ}$  initiates the auto-zero phase by driving both switches into Position 1. The inputs of the nulling amplifier, consisting of multiple amplifier stages itself, are shorted together, while its output is connected to capacitor  $C_1$ . In this configuration,  $A_N$  measures its own input offset voltage and stores it on  $C_1$ . Mathematically we can express the voltage at  $C_1$  as  $V_{C1} = G_B(A_{IN}V_{OSN} - A_ZV_{C1})$  which, by simple rearrangement, is shown as Equation 1.

$$(EQ. 1) \quad V_{C1} = V_{OSN} \frac{G_B A_{IN}}{1 + G_B A_Z}$$

In the amplification phase, OSC drives both switches into Position 2 (Figure 2). In this configuration,  $A_N$  amplifies  $V_{C1}$  by the factor  $A_Z$ , subtracts it from the amplified differential input signal ( $A_{IN}(V_{OSN} + V_{ID})$ ) and charges capacitor  $C_2$  with the amplified difference to  $V_{C2} = G_B [A_{IN}(V_{OSN} + V_{ID}) - A_ZV_{C1}]$ . Substituting  $V_{C1}$  with Equation 1 and solving for  $V_{C2}$  results in Equation 2.

$$(EQ. 2) \quad V_{C2} = G_B A_{IN} V_{ID} + V_{OSN} \frac{G_B A_{IN}}{1 + G_B A_Z}$$

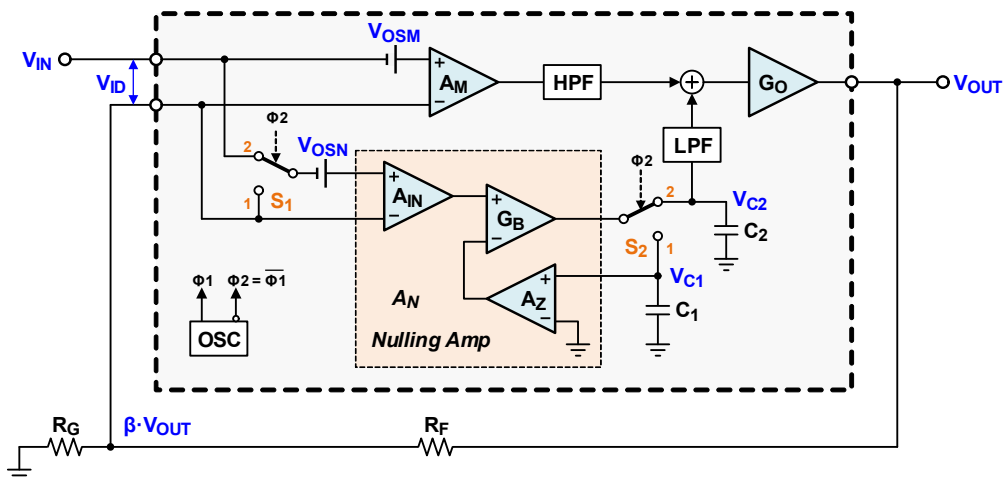


Figure 2. ISL28134: Amplification Phase

At the same time, the main amplifier amplifies its differential input to produce  $A_M(V_{ID} + V_{OSM})$  at its output. The sum of both voltages is then amplified by the output gain stage ( $G_O$ ) to produce an output voltage of:

$$V_{OUT} = G_O [V_{C2} + A_M(V_{ID} + V_{OSM})]$$

Substituting  $V_{C2}$  with [Equation 2](#) then yields [Equation 3](#):

$$(EQ. 3) \quad V_{OUT} = G_O (G_B A_{IN} + A_M) V_{ID} + G_O A_M V_{OSM} + \frac{G_O G_B A_{IN}}{1 + G_B A_Z} V_{OSN}$$

With the auto-zero architecture being optimized such that  $A_M = A_{IN}$  and all gain stages being much larger than 1, [Equation 3](#) can be simplified to:

$$V_{OUT} = G_O A_{IN} G_B V_{ID} + G_O A_{IN} V_{OSM} + \frac{G_O A_{IN}}{A_Z} V_{OSN}$$

Then, factoring out the gain factor of the  $V_{ID}$ ,  $G_O A_{IN} G_B$ , presents  $V_{OUT}$  in the form of the generic amplifier equation:

$$(EQ. 4) \quad V_{OUT} = G_O A_{IN} G_B \left( V_{ID} + \frac{V_{OSM} + V_{OSN}/A_Z}{G_B} \right)$$

The equation for the generic amplifier in [Figure 3](#) is:

$$(EQ. 5) \quad V_{OUT} = A_{OL} (V_{ID} + V_{OS-Eff})$$

where  $A_{OL}$  is the open-loop gain of the amplifier and  $V_{OS-Eff}$  its effective offset voltage.

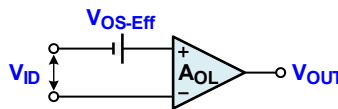


**Figure 3. Generic Amplifier with Effective Offset**

Comparing [Equation 4](#) with [Equation 5](#) shows that the effective open-loop gain of the auto-zero amplifier is

$$A_{OL} = G_O A_{IN} G_B \text{ and its effective offset is } V_{OS-Eff} = \frac{V_{OSM} + V_{OSN}/A_Z}{G_B}$$

Therefore, the offset voltage of the main is reduced by the gain  $G_B$  and the offset of the nulling amplifier by  $G_B \cdot A_Z$ . If we consider the open-loop gains of the various gain stages to be in the region of 10000 or higher, it becomes evident that even an inherent offset voltage of several millivolts is reduced to an effective input offset voltage of microvolts for the complete auto-zero amplifier.

## 2. Noise Reduction in the Frequency Domain

The amplifier structures in [Figures 1](#) and [2](#) show a low-pass filter (LPF) that is transparent to the auto-zeroing process, but necessary to filter out high-frequency components created by the switching process during auto-zeroing. Because the auto-zero amplifier constitutes a sampled data system, the process of sampling generates frequencies consisting of the sum and difference of the input signal frequency ( $f_{IN}$ ) and the auto-zero clock frequency ( $f_{AZ}$ ).

[Figure 4](#) depicts the process of noise reduction by demonstrating the effects of sampling in the frequency domain. The sampling of the input signal constitutes a modulation, with  $f_{AZ}$  as the carrier, and  $V_{IN}$  (or  $f_{IN}$ ) as the modulating signal. Both switches, S1 and S2, are replaced by the modulators, M1 and M2.  $V_{M1}(f)$  in [Figure 4](#) shows that the first modulation of  $V_{IN}$  causes sidebands of  $f_{IN}$  on both sides of the odd harmonics of  $f_{AZ}$ .

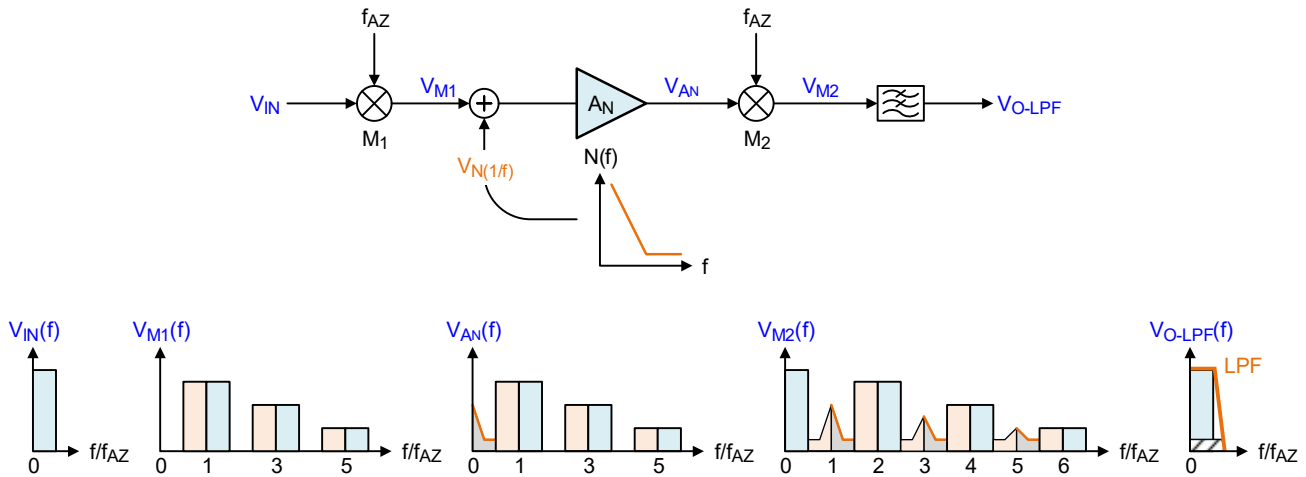


Figure 4. Auto-Zeroing in the Frequency Domain

The amplitudes of the sidebands decrease following a  $1/n$  function, with  $n$  indicating the order of the harmonic. The  $1/f$  noise of  $A_N$  present in the baseband adds to the modulated input signal after the first modulation stage (see  $V_{AN}(f)$ ). The combined signal is amplified by  $A_N$  and fed into the demodulator,  $M_2$ . The  $1/f$  noise, experiencing its first modulation through  $M_2$ , introduces sidebands on both sides of the odd harmonics of  $f_{AZ}$ . For the already modulated input signal ( $V_{M1}$ ) however,  $M_2$  represents the second modulating stage.

This second modulation transforms  $f_{IN}$  to even higher frequencies, causing sidebands around the even harmonics of  $f_{AZ}$  as well as around the origin. Therefore, the input signal reappears in the baseband. The second modulation, therefore, constitutes the demodulation of  $f_{IN}$ . Applying a higher-order low-pass filter, whose steep roll-off limits the baseband to frequencies well below  $f_{AZ}$ , also reduces the noise drastically.

Figure 5 shows the spectral noise density of the ISL28134 in comparison with that of a precision CMOS op-amp. The noise is virtually flat across the entire frequency range, except for the narrow noise around 10kHz.

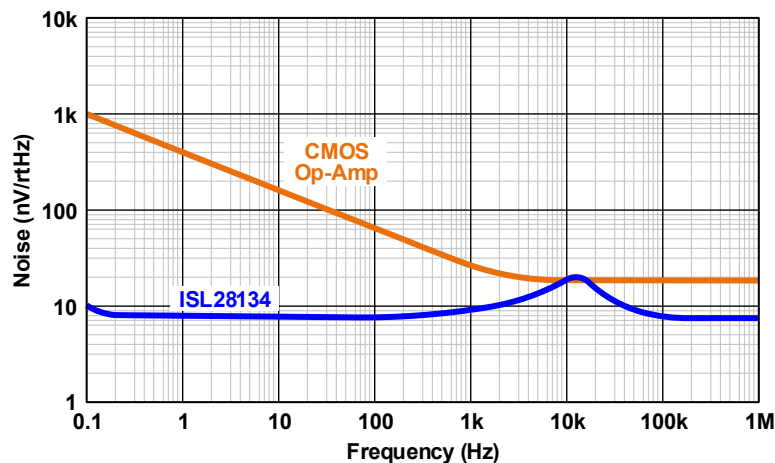


Figure 5. Spectral Noise Density

### 3. Applications

#### 3.1 Thermocouple Amplifier

The temperature measurement circuit in [Figure 6](#) is a low-frequency application that allows the ISL28134 to be switched directly into the signal path. A precision voltage reference (ISL21010-41) provides the 4.096V bridge supply. The forward voltage of diode  $D_1$  has a negative temperature coefficient of  $-2\text{mV}/^\circ\text{C}$  and provides cold junction compensation using the resistor network  $R_1$  to  $R_3$ .

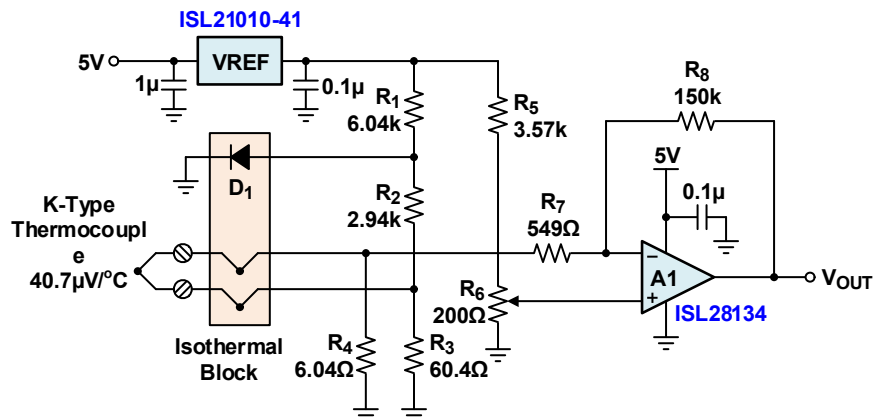


Figure 6. Temperature Measurement with Thermocouple

The zero adjustment for a defined minimum temperature is achieved using  $R_6$ , while  $R_7$  and  $R_8$  set the gain for the output amplifier. The single-supply amplifier providing an open-loop gain of 174dB allows 16-bit or better accuracy at high gain in low-voltage applications. Auto-zeroing removes  $1/f$  noise and provides typical values of  $0.2\mu\text{V}$  of input offset and  $0.5\text{nV}/^\circ\text{C}$  of offset drift over temperature. Therefore, auto-zero amplifiers ideally suit single-supply precision applications where high accuracy, low drift, and low noise are imperative.

#### 3.2 Active Low-Pass Filter

The third-order low-pass filter in [Figure 7](#) has a corner frequency of 200kHz, which is twice the auto-zero clock frequency. Aliasing and intermodulation noises are highly attenuated, which permits input signal operation across its entire gain bandwidth. In addition, the output of the amplifier provides rail-to-rail drive capability, allowing for a high signal-to-noise ratio at low supply voltages.

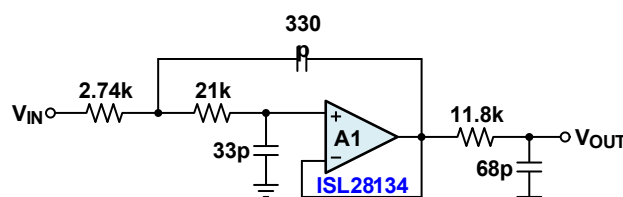


Figure 7. 200kHz 3rd Order Low-pass Filter

#### 3.3 Wideband Amplifier

In wideband applications with bandwidths in the tens of megahertz, the ISL28134 provides DC accuracy to a wideband amplifier. [Figure 8](#) shows the required circuit configuration in the form of a composite amplifier design.

The ISL28134 functions as an integrator operating in the bias path of the wideband amplifier. The signal path still runs from  $V_{IN}$  through  $R_G$  and  $R_F$  to  $V_{OUT}$ . The integrator has two functions. At low frequencies, it provides high gain to the offset-cancellation loop, reducing the input offset of the wideband amplifier down to the input offset of the auto-zero amplifier. At high frequencies, a large time constant ( $R_{INT}$ ,  $C_{INT}$ ) ensures that the closed-loop gain of the integrator quickly decreases to prevent the signal transfer to the non-inverting input of the wideband amplifier.

**Note:** The input noise of the amplifier is amplified by the non-inverting closed-loop gain of the integrator. Therefore, at high frequencies, the ISL28134 operates as a voltage follower (gain = 1), passing its input noise on

to the wideband amplifier. To eliminate this noise, a low-pass filter ( $R_{LPF}$ ,  $C_{LPF}$ ) with low-frequency cutoff is added to the output of the ISL28134.

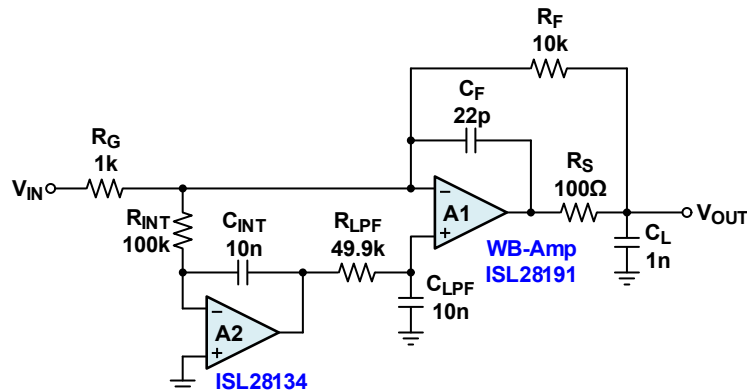


Figure 8. Auto-Zeroed Wideband Amplifier

In this application, A1 drives a large load capacitance ( $C_L$ ), which interacts with the output impedance of A1 ( $R_O$ ). To preserve stability, resistor  $R_S$  is implemented to isolate  $C_L$  from A1. The output ( $V_{OUT}$ ) of the resulting low-pass filter has a -3dB cut-off at  $f_{-3dB} = 1/[2\pi(R_O+R_S)C_L]$ . However, the phase correction due to  $R_S$  works only at low frequencies. For high-frequency stability, a second feedback loop using  $C_F$  is implemented that compensates the phase lag of the low-pass filter at the output of A1. The values of  $R_S$  and  $C_F$  are calculated with:

$$R_S = R_O \cdot \frac{R_F}{R_G}$$

and

$$C_F = C_L \left( \frac{R_O + R_S}{R_F} \right) \cdot \left( 1 + \frac{R_G}{R_F} \right)$$

### 3.4 High-Gain Amplifier

When designing a high-gain amplifier (Figure 9), care must be taken to maintain the input impedance below a certain value. The input stage of Auto-Zero Amplifiers (AZA) does not behave like conventional amplifier input stages. An AZA uses switches at the amplifier input that continually samples the input signal at 100kHz to reduce the input offset voltage down to microvolts. The dynamic behavior of these switches induces charge injection currents to the input terminals of the amplifier. These currents have a DC path to ground through the resistances seen at the input terminals. Therefore, input impedances larger than 10kΩ cause the bias currents to increase significantly. To minimize this effect, an input resistance of <10kΩ is recommended.

Also, match the input impedance between the IN+ and IN- terminals to minimize the input offset voltage due to bias current. This offset current causes as an additional input offset voltage,  $I_{OS} \cdot R_{IN}$ .

For a 10000V/V (80dB) gain amplifier using a 1MΩ feedback resistor, a total input offset current of 500pA generates an additional output offset voltage of 0.5mV. By keeping the input impedance low and balanced across the amplifier inputs, this current is kept below 100pA and its associated offset reduced to ≤0.1mV.

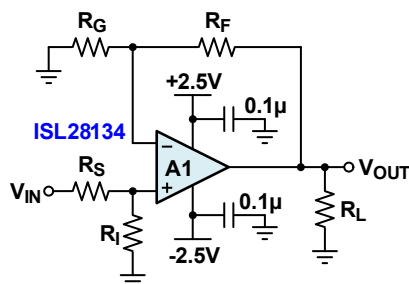
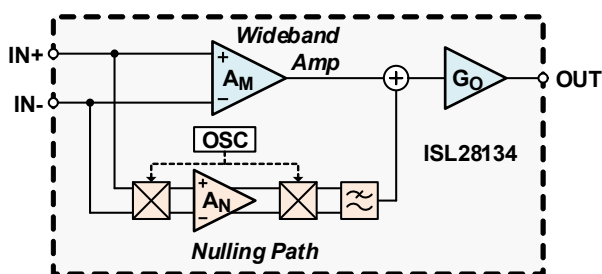


Figure 9. Making  $R_S || R_I = R_F || R_G$  Reduces Input Offset Voltage Due to Bias Currents

### 4. Conclusion

The ISL28134 is ideal for amplifying the sensor signals of analog front-ends that include pressure, temperature, medical, strain gauge, and inertial sensors down to the  $\mu\text{V}$  levels. The ISL28134 can be used over standard amplifiers with high stability across the full industrial temperature range of  $-40^\circ\text{C}$  to  $+125^\circ\text{C}$ . [Figure 10](#) shows the device block diagram and a summary of its main features.



Low input offset voltage	0.2 $\mu\text{V}$
<b>Low offset drift</b>	0.5nV/ $^\circ\text{C}$
High gain-bandwidth product	3.5MHz
Low voltage noise	0.8nV/ $\sqrt{\text{Hz}}$
Wide supply voltage range	2.2V to 5.5V
<b>Low supply current</b>	675 $\mu\text{A}$
<b>Voltage swing</b>	R-R/IO
Wide temperature range	$-40^\circ\text{C}$ to $125^\circ\text{C}$

Figure 10. ISL28134: Block Diagram and Key Features

### 5. Revision History

Rev.	Date	Description
1.00	Apr.1.20	Initial release

## IMPORTANT NOTICE AND DISCLAIMER

RENESAS ELECTRONICS CORPORATION AND ITS SUBSIDIARIES (“RENESAS”) PROVIDES TECHNICAL SPECIFICATIONS AND RELIABILITY DATA (INCLUDING DATASHEETS), DESIGN RESOURCES (INCLUDING REFERENCE DESIGNS), APPLICATION OR OTHER DESIGN ADVICE, WEB TOOLS, SAFETY INFORMATION, AND OTHER RESOURCES “AS IS” AND WITH ALL FAULTS, AND DISCLAIMS ALL WARRANTIES, EXPRESS OR IMPLIED, INCLUDING, WITHOUT LIMITATION, ANY IMPLIED WARRANTIES OF MERCHANTABILITY, FITNESS FOR A PARTICULAR PURPOSE, OR NON-INFRINGEMENT OF THIRD PARTY INTELLECTUAL PROPERTY RIGHTS.

These resources are intended for developers skilled in the art designing with Renesas products. You are solely responsible for (1) selecting the appropriate products for your application, (2) designing, validating, and testing your application, and (3) ensuring your application meets applicable standards, and any other safety, security, or other requirements. These resources are subject to change without notice. Renesas grants you permission to use these resources only for development of an application that uses Renesas products. Other reproduction or use of these resources is strictly prohibited. No license is granted to any other Renesas intellectual property or to any third party intellectual property. Renesas disclaims responsibility for, and you will fully indemnify Renesas and its representatives against, any claims, damages, costs, losses, or liabilities arising out of your use of these resources. Renesas' products are provided only subject to Renesas' Terms and Conditions of Sale or other applicable terms agreed to in writing. No use of any Renesas resources expands or otherwise alters any applicable warranties or warranty disclaimers for these products.

(Rev.1.0 Mar 2020)

### Corporate Headquarters

TOYOSU FORESIA, 3-2-24 Toyosu,  
Koto-ku, Tokyo 135-0061, Japan  
[www.renesas.com](http://www.renesas.com)

### Contact Information

For further information on a product, technology, the most up-to-date version of a document, or your nearest sales office, please visit:  
[www.renesas.com/contact/](http://www.renesas.com/contact/)

### Trademarks

Renesas and the Renesas logo are trademarks of Renesas Electronics Corporation. All trademarks and registered trademarks are the property of their respective owners.